J. Basic. Appl. Sci. Res., 3(6)973-987, 2013
© 2013, TextRoad Publication
ISSN 2090-4304
Journal of Basic and Applied Scientific Research
www.textroad.com

Combined Simulation of Air Flow, Radiation, Moisture Transport around a Person in a Ventilated Room in ordet to Minimize Energy Consumption

Nabi Jahantigh[1], Masoud Mirzaei[2], Ali Keshavarz[3], Ali Hosieni[4]

Mechanical engineering faculty, K. N. Toosi University of Technology, Vanak Sq. Mollasadra St., P.O.B. 19395-1999, Tehran, Iran
[1]Ph. D. student of mechanical engineering
[2] Associated professor of Aerospace engineering
[3]Associated professor of mechanical engineering
[4]M.S student of mechanical engineering

ABSTRACT

One of the conventional indoor heating systems is the convective heating type. In such systems, besides the types of materials used in the building, air flow parameters, size and position of the inlet and outlet vent have great influence on the thermal comfort conditions. In this study the effects of physical and geometrical flow parameters such as cross section area, velocity, and position of inlet and outlet vent, temperature and humidity of the ambient in order to achieve the best of PMV (Predicted Mean Vote) with minimized consumption of energy has been carried out. A three-dimensional CFD code is used to solve the air flow field and mass transfer around a virtual manikin of a real stand physiological located in the center of a residential room. The velocity and temperature of the air flow at the inlet varies in the range of 0.1- 1 m/s, and 22-45℃, respectively. Numerical results have a good agreement with the experimental data reported in the literature. The optimal size and the location of the inlet and outlet are determined with the consideration of thermal and architecture limitations. With the selection of proper location of inlet and outlet vents, variations of temperature and velocity cause significant effects on the thermal comfort and energy consumption. The inlet velocity increment causes the thermal comfort to be achieved at lower temperatures which in turn reduces the consumption of energy. Also, a better symmetrical velocity distribution around the manikin is presented in this case. At the proper position, the relative humidity be decreased and also the required velocity be reduced to provide the thermal comfort. Lower velocity makes lower heat losses through the walls and manikin segments up to 25 % which eventually reduces the energy consumption

KEYWORDS: Virtual Manikin, Thermal comfort, CFD analyzing, heat transfer, Energy Consumption Decrease.

Nomenclature:

ρ	Density	$\vec{V}$	Velocity vector
S_m	Any source term	$\vec{g}$	Gravitational acceleration
$\vec{F}$	External body force	$\bar{\bar{\tau}}$	Stress tensor
μ	Molecular viscosity	I	Unit tensor
k_{eff}	Effective conductivity	k_t	Turbulent thermal conductivity
E	Total energy (J)	S_h	Any volumetric heat source
h	Sensible enthalpy	$\vec{J_j}$	Diffusion flux of species
c_p	Heat capacity at constant pressure, volume	Y_j	Mass fraction of species
μ_t	Turbulent viscosity	$D_{j,m}$	Mass diffusion coefficient for species
PMV	Predict mean vote	D_T	Turbulent diffusivity
M	Metabolic heat production (w/m^2)	L	The heat load of the body
W	External work(w/m^2)	R	Radiative heat loss(w/m^2)
S	Heat storage(w\m^2)	C	Convective heat loss(w/m^2)
E_{sk}	Evaporative heat loss of skin	C_{res}	Convection heat loss due to respiration(w/m2)
E_{res}	Evaporative heat loss due to respiration(w/m2)	P_a	ambient pressure air (kpa)
$R_{e,cl}$	Resistance of clothes	F_{cl}	Coefficient of the clothes
K_{cl}	heat transfer due to the clothes	t_{cl}	Temperature of the clothes
$\bar{t}_r$	Radiation Mean temperature	t_s	Environment temperature

1. INTRODUCTION

The conventional heating and cooling systems for indoor environment are convective heating and cooling systems. In such systems temperature, humidity and velocity of the inflow air, the cross sections and locations of the inlet and outlet influence on the comfort. Moreover the position of the doors and windows, their materials and heat transfer characteristics of the environment are all the factors that affect on a person's thermal comfort

*Corresponding Author: Masoud Mirzaei, Associated professor of Aerospace engineering, email: mirzaie@kntu.ac.ir

and flow distribution in an environment. There are many complexities to achieve the proper heat and flow distributions in order to reach thermal comfort. Therefore in the studies that have been conducted so far, a great simplification has been considered. However, nowadays, with the advances of computational resources, solving of three dimensional air flows without previous simplification has become possible.

One of the first CFD studies that could predict the flow and thermal indoor conditions was conducted by Nielsen [1]. He calculated the distribution of temperature and heat transfer in a room in the absence of the virtual model in a room. Later, Gan used a CFD to assess the room thermal conditions in the presence of a virtual manikin [2]. Murakami S. has developed virtual thermal model to predict the thermal comfort, air flow effects, radiation and perspiration from the body surface [3]. He achieved the radiation heat transfer coefficients between the body and the environment for undressed and dressed states. Kurazumi obtained free convective and radiative heat transfer coefficients between the body and the environment [4].

Another important factor affecting the flow field, heat transfer and thermal comfort in indoor environments is the form of the body. The physiological form of the body has a large effect on the flow distribution around a person. Body affects the pressure gradient near the body and changes the air velocity around itself. This change in the velocity has a direct effect on increasing the heat transfer from the body surface. Therefore, ignoring the form of the body and using equivalent surfaces has created numerous errors in the previous studies [5]. Kilic and Sevilgen assessed the local heat transfer of a body in a room by considering the physiological form of the body [6].

So far, the effects of each of the flow and geometric factors on thermal comfort have been studied individually in previous studies. The experimental evaluation of simultaneous interaction of these parameters is costly and difficult. However using numerical techniques, simultaneous interaction of these parameters can be estimated.

It is noteworthy that in previous studies the effects of changes in temperature, humidity, area and position of the inlet and outlet interactions have not been studied. However, in this study, in addition to solving the flow field around the human in order to reach thermal comfort, the changes in the inlet and outlet area, humidity, temperature, and velocity have been investigated. A parametric study on the influential parameters to reach lower energy consumption and thermal comfort conditions has been done. The physiological form of the proposed model is fully compatible with that of the human body. The cross sections of the inlet and outlet vary in from 0.1 m^2, to the maximum possible value depending on the dimension of the room. The air inlet velocity and temperature can change from 0.1 5 to 1 m/ s and 20 to 45 ° C, respectively. These limits are chosen based on the inlet temperature becoming higher, equal or less than the volume-average of the room temperature. Using the CFD code, the heat and mass transfer and flow distribution in a room with a virtual manikin located at the center of the room, have been assessed. Moreover, the location of the inlet and outlet vents, air velocity and temperature are determined in order to reach the thermal comfort. However, this item has not been reported by other researchers.

Governing equations and Solutions

The governing equations of this flow field are continuity, momentum, energy and mass transfer. Along these equations, radiation and turbulence modeling equations are to be solved in this problem.

Continuity equation is as follows [7]:

$$\frac{\partial \rho}{\partial t} + \nabla.\left(\rho \vec{V}\right) = S_m \tag{1}$$

Equation (1) is the general form of the mass conservation and is valid for incompressible and compressible flows. The source S_m is considered zero.

Conservation of momentum in an inertial (non-accelerating) reference frame is described as [8].

$$\frac{\partial}{\partial t}\left(\rho \vec{V}\right) + \nabla.\left(\rho.\vec{V}.\vec{V}\right) = -\nabla p + \nabla.(\bar{\bar{\tau}}) + \rho\vec{g} + \vec{F} \tag{2}$$

Where p is the static pressure, $\bar{\bar{\tau}}$ is the stress tensor, and $\rho\vec{g}$ and $\vec{F}$ are the gravitational body force and external body, respectively.

The stress tensor $\bar{\bar{\tau}}$ is given by

$$\bar{\bar{\tau}} = \mu\left[\left(\nabla\vec{V} + \nabla\vec{V}^T\right) - \frac{2}{3}\nabla.\vec{V}I\right] \tag{3}$$

Where μ is the molecular viscosity, I is the unit tensor, and the second term on the right hand side is the effect of volume dilation.

The energy equation is in the following form:

$$\frac{\partial}{\partial t}(\rho E) + \nabla.\left(\vec{V}(\rho E + p)\right) = \nabla.\left(k_{eff}\nabla T - \sum_j h_j\vec{J_j} + (\bar{\bar{\tau}}_{eff}.\vec{V})\right) + S_h \tag{4}$$

Where k_{eff} is the effective conductivity ($k + k_t$, where k_t is the turbulent thermal conductivity), and $\vec{J_j}$ is the diffusion flux of species j. The first three terms on the right-hand side of Equation 4 represent energy transfer

due to conduction, species diffusion, and viscous dissipation, respectively. S_h term includes any volumetric heat source. In Equation 4,

$$E = h - \frac{p}{\rho} + \frac{V^2}{2} \quad (5)$$

Where sensible enthalpy h is defined for incompressible flows as

$$h = \sum_j Y_j h_j + \frac{p}{\rho} \quad (6)$$

In Equation 6, Y_j is the mass fraction of species j and

$$h_j = \int_{T_{ref}}^{T} C_{p,j}\, dT \quad (7)$$

Here T_{ref} is 298.15 K.

The conservation equation for the species transport in the general form is:

$$\frac{\partial}{\partial t}(\rho Y_j) + \nabla.(\rho \vec{V} Y_j) = \nabla.\vec{J}_j + S_j \quad (8)$$

Where S_j is any defined source terms.

In turbulent flows, the mass diffusion in the following form is computed:

$$\vec{J}_j = -\left(\rho D_{j,m} + \frac{\mu_t}{Sc_t}\right)\nabla Y_j - D_{T,j}\frac{\nabla T}{T} \quad (9)$$

Here, $D_{j,m}$ is the mass diffusion coefficient for species j in the mixture, and $D_{T,j}$ is the thermal (Soret) diffusion coefficient.

Where Sc_t is the turbulent Schmidt number ($\frac{\mu_t}{\rho D_t}$ where μ_t is the turbulent viscosity and D_T is the turbulent diffusivity).

PMV is calculated to predict the response of large groups of people to the thermal comfort that can be expressed as: [9].

$$PMV = (0.303\exp(-0.035M) + 0.028)L \quad (10)$$

Where M is the metabolic rate and L is the heat load of the body that is considered as the difference between heat generation and dissipation of the body. The body surface temperature and activity level of the person are assumed to be constant. The heat balance equation is as follows:

$$S = M \mp W \mp R \mp C \mp K - E_{sk} - (C_{res} + E_{res}) \quad (11)$$

All terms in equation 11 are determined by solving the flow field.

When $S = 0$, the thermal equilibrium will be satisfied [8]. In equation 11 E_{sk}, C_{res} and E_{res} terms can be calculated as follow:

$$E_{sk} = \frac{w(p_{sk,s} - p_a)}{R_{e,cl} + 1/(F_{cl}h)} \quad (12)$$

$$C_{res} = 0.0014\, M(34 - T_a) \quad (13)$$

$$E_{res} = 1.72 \times 10^{-5} M(5867 - P_a) \quad (14)$$

The heat transfer from the cover (K_{cl}) is calculated as:

$$K_{cl} = \frac{t_s - t_{cl}}{0.155 I_{cl}} \quad (15)$$

By solving the flow field, the thermal radiation exchange between the surfaces of the body and environmental surfaces are calculated, also the equation (16) can be used.

$$R = f_{cl} h_r (t_{cl} - \bar{t}_r) \quad (16)$$

Some of the surfaces, such as the surface between the body and arms or the surface between the legs, do not exchange any radiation with the environment, but have heat exchange with other surfaces of the body. So the effective heat exchanging surface is less than the surface of the body. These effects will be taken into account by applying the coefficient of f_{eff}. Experimental studies recommend 0.696 for sitting and 0.725 for standing states.

By solving the flow field, the convection flux is obtained. The amount of heat transfer can be obtained as:

$$C = f_{cl} h_c (t_{cl} - t_a) \quad (17)$$

Where h_c for free convection is:

$$h_c = 2.38(t_{cl} - t_a)^{0.25} \quad (18)$$

And for force convection is:

$$h_c = 12.1\sqrt{v_{ar}} \quad (19)$$

In order to solve the flow field, a 3D computational code for steady state was used. PISO algorithm has been used to resolve the coupling velocity-pressure. When second-order accuracy is desired, quantities at cell faces

are computed using a multidimensional linear reconstruction approach [10]. Pressure discretization is done by second order method to achieve high accuracy. The RNG $k-\varepsilon$ model is used as the turbulence model of the problem.

Heating surfaces and heat sources due to radiation within the fluid are included in the model using the DO radiation model. The DO model spans the entire range of optical thicknesses. It also allows the solution of radiation at semi-transparent walls.

Geometry of the problem

Room geometric model is shown in Figure 1. The model is composed of a room with a standard 3×4×4 meters, in which a virtual manikin with real dimensions is placed at the center. A window on the south wall and a door on the south wall are also placed. In order to supply heat transfer and air flow in the room, an inlet and an outlet with dimensions 760 × 120 mm are mounted on the walls. They can be placed at any location on the side walls of the room.

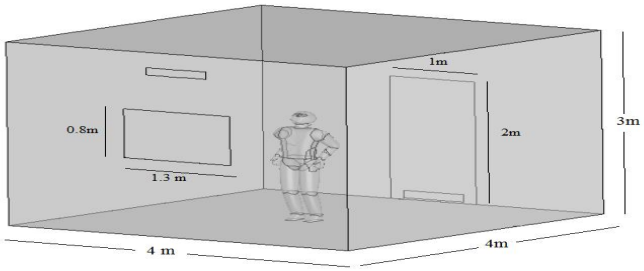

Figure 1: Room geometric model and dimension

The Manikin with the height of 1.81 m. and the total body surface area of 2.315 m^2 is divided into 22 different parts, each named for the area that can be seen in Figure 2.

number	The name of area	area	number	number	
1	Head	0.566	12	Left foot	0.0666
2	Neck	0.0212	13	Right foot	0.666
3	Left shoulder	0.0287	14	Right leg	0.1097
4	Left Arm	0.0987	15	Right thigh	0.2794
5	Waist	0.1358	16	Basin	0.0905
6	Left hand	0.0278	17	Right hand	0.0278
7	Left forearm	0.0964	18	Right forearm	0.0964
8	Left hand	0.452	19	Bowl	0.1019
9	Pelvis	0.0679	20	Brisket	0.1698
10	Left thigh	0.2794	21	Right arm	0.0987
11	Left leg	22	22	Right shoulder	0.0287
Total area	2.3104				

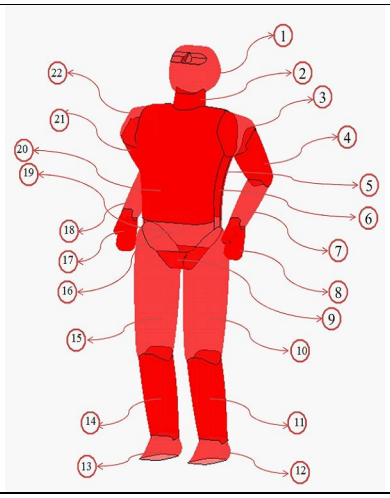

Figure 2: The segment of the manikin model

Computational grid

Since we are dealing with a complex geometry and very small surfaces in this problem the generation of the structured grid for all the sub regions is not possible so here we have used a combination of unstructured-structured grid system. First the surface of manikin is covered with triangle grid. This type of grid has the ability to cover the smallest surface of the model. Then, the space between the model, the room and the thermal heater is filled with a grid system using the Algorithm T-Grid. The computational domain at z=0 in the room is shown in figure 3. Since the flow field around the person includes high gradients of flow parameters, the size of the grid around the person should be fine. An appropriate distribution function starting from the marginal layer around the surface and continuing at maximum step can be used. The study was conducted to show the grid independence from of the results. The problem was solved in several grid size systems and the results became grid independence for a grid system with 3900000. This study was shown in Figure 4

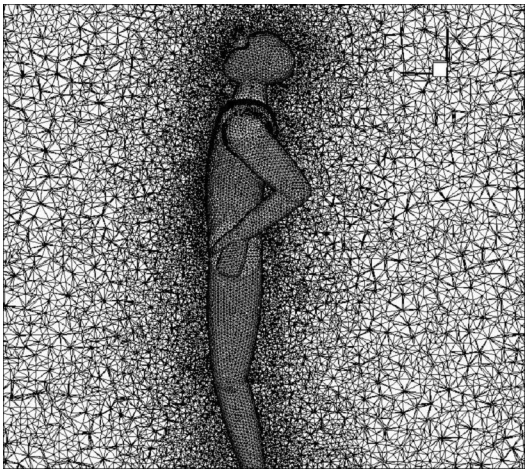

Figure 3: The computational domain at z=0 in the room

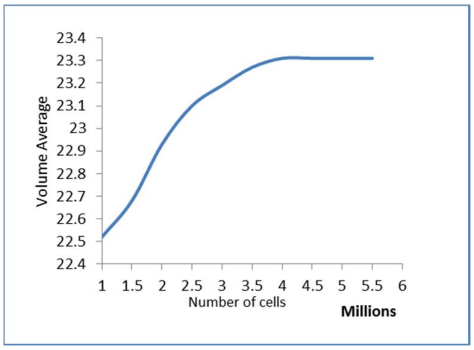

Figure 4: the effects of the cell number to the volume temperature of room

Boundary Conditions

For this problem the following boundary conditions were employed:

1. Thermal boundary conditions on the manikin surface
2. Boundary conditions on the walls and the inlet and outlet

The temperature of the surface area of the manikin depends on the temperature of the interior of the body. The surface temperature of the manikin for dressed parts such as hands and legs is 33.1 ° C and for the undressed parts is 33.7 ° C [11]. In addition to body heat exchange with the environment, it has humidity exchange too. In order to model this exchange, a mass fraction of water in the skin has been considered as $10\,gH_2O/kgAir$. The walls of the room are made of dense brick, and all of the walls except the wall containing window, have been considered isolated. Physical characteristics of the walls, doors and windows are shown in Table 1. The wall containing window and window themselves have been exchanging heat with their surroundings. The heat transfer coefficient between the wall and the surrounding area is considered to be $25\,W/m^2$ [11] and the free stream temperature is 0° C. the internal walls emissivity coefficient is 0.95. At the inlet vent, the boundary conditions is velocity inlet and the velocity varies from 0.15 to 1 m/s. Inlet air temperature varies from 20 to 45 °C. To ensure proper humidity, water vapor mass fraction at the inlet is considered as $9.5\,gH_2O/Kg\,Air$. The boundary condition at the outlet vent is considered as the pressure outlet, and the gage pressure is zero Pascal. Considering the standard of ASHRAE2000,the metabolic rate that is equal to this posture is 104.6 [9]. The temperature of the floor is $25℃$..The thickness of the walls and ceiling is 0.25 m. the Door is made of wood and it has a heat transfer coefficient of $h = 15\,w/m.K$. the emissivity coefficient value for the body has been considered as 0.98 [9].

Table 1: Physical characteristic of the wall, door and window

	Door	Wall	Window
width	50	250	25
ρ kg/m^3	700	1940	840
C_p $kj/(kg-°K)$	2.31	0.84	0.84
K $w/m^2.°K$	0.173	0.06	0.2
ϵ	0.9	0.95	0.8

RESULTS AND DISCUSSIONS

Validation of Results

The present results are compared with numerical and experimental data reported in [6]. The results have good accuracy in comparison with those reported by [6]. The flow rate, relative humidity and temperature were measured at various points located on top of the body are reported in Figures 5, 6 and 7. In these figures, the results are compared with the data presented in [6]. As Figure 5 shows the maximum difference between the experimental and numerical data of [6], does not go beyond 0.03 m/s. The comparison between the calculated temperature and relative humidity emphasizes high accuracy of the results. The maximum difference between the calculated temperature with experimental and numerical data of [6] is about0.3 and 0.4℃. These values are about 0.5% for relative humidity.

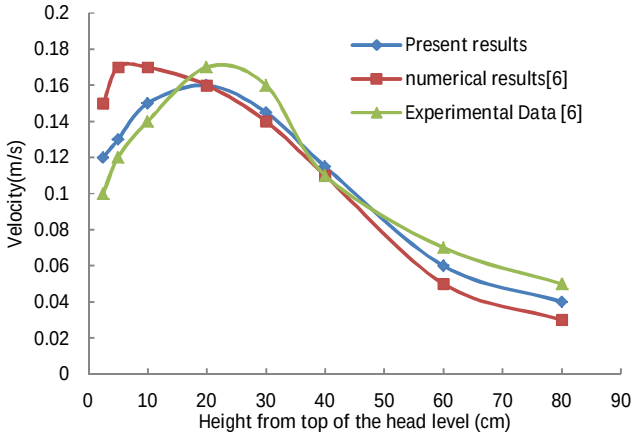

Figure 5: Comparison the computed velocity with numerical and experimental results of ref. [6]

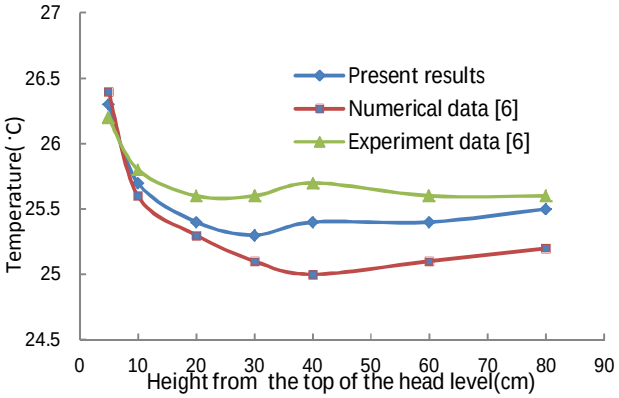

Figure 6: Comparison the computed temperature with numerical and experimental results of ref. [6]

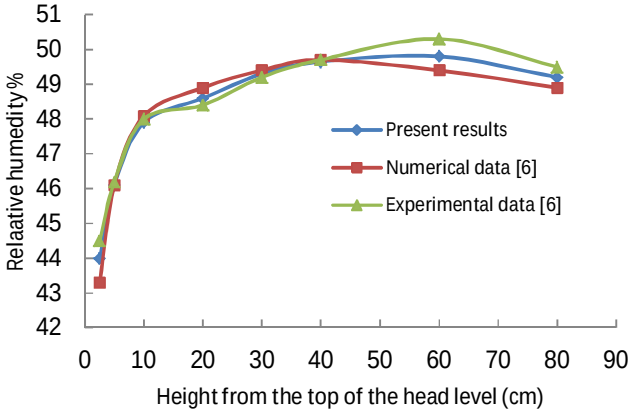

Figure 7: Comparison the computed RH% with numerical and experimental results of ref. [6]

The effect of inlet and outlet vents locations on the results

The locations of inlet and outlet vents relay to each other concern with several limitations. The first limitation is the architecture of the space that does not allow the inlet and outlet to be placed at any point of the space. Therefore, the inlet and outlet should be located only at the minimum and maximum heights. The other limitation is the stagnation region in the space. The stagnation region is the area containing zero-velocity air. According to Figure 4 when the inlet and outlet vents are located in a vertical direction or in a direction other than that of the middle of the walls, more stagnation areas are created in the room. To overcome this problem, the position in front of each of the vents is avoided.

The effects of the positioning in the vertical direction on the results

In the following Table, several cases have been considered

Table 2: The different case studies

Cases	Location of inlet	Location of outlet	Inlet temperature condition
Case 1	at the highest level	at the lowest level	lower than the volume-averaged temperature of the room
Case 2	at the lowest level	at the highest level	higher than the volume-averaged temperature of the room
Case 3	at the highest level	at the lowest level	higher than the volume-averaged temperature of the room
Case 4	at the lowest level	at the highest level	Lower than the volume-averaged temperature of the room

The inlet flow rate is constant. The results are presented in Table 3.

Table 3: the comparison between flow characteristic in different cases

	T_{in} ℃	V_{in} m/s	T_{mrt} ℃	T_{ave} ℃	Re Hu_{ave} %	PMV
Case 1	23	0.15	23.05	23.32	56.92	-0.61
Case 2	30	0.15	23.39	24.02	52.15	-0.34
Case 3	30	0.15	23.59	24.23	53.68	-0.28
Case 4	23	0.15	23.07	23.31	54.57	-0.6

The volume-averaged temperature of the room in all cases is almost the same, and the maximum difference is 0.21 ° C. This amount for the average radiation temperature is in the same value, and the maximum is 0.20 ° C. The PMV for the case 1, 4, 2 and 3 is -0.61, -0.60, - 0.34 and -0.28, respectively. As it is observed, there is no significant difference in these values. As shown in Table 4 in both cases 1and 3 the relative humidity is much higher than that of both cases 2 and 3.

Table 4: Result for displacement of the inlet and outlet in the longitudinal direction

No	T_{ave} ℃	T_{mrt} ℃	$Re\ Hu_{ave}$ %	$q_r\ W/m^2$	$q_c\ W/m^2$	$q_{res}\ W/m^2$	$E_{res}\ W/m^2$	$E_{sk}\ W/m^2$	PMV
1	23.38	23.05	56.92	35.94	44.02	1.50	5.08	30.92	-0.61
2	23.31	23.07	54.57	35.87	43.87	1.50	5.19	30.99	-0.61
3	23.43	23.14	54.18	35.64	43.58	1.48	5.14	30.59	-0.58
4	23.29	23.09	54.58	35.81	44.31	1.50	5.17	31.34	-0.63
5	23.18	23.17	54.01	35.55	43.97	1.50	5.13	30.83	-0.61
6	23.24	23.14	54.18	35.89	44.14	1.49	5.11	30.12	-.60

When the inlet temperature is lower than the volume-averaged temperature and inlet is at the highest level, the inlet air due to more density has no tendency to move to the top. So, the relative humidity increment is restricted to lower areas of the room. When the inlet temperature is lower than the volume-averaged temperature and the inlet is at the highest level, this higher density air moves downwards and decreases the relative humidity.

When the inlet temperature be higher than the volume-averaged temperature, and the inlet is at the lowest level the air with lower density and lower humidity moves to the upper regions, and reduces the humidity, but when the inlet vent is at the highest level the warm and dry inlet air is confined to the same area and the relative humidity increases. The contours of temperature, the velocity, and relative humidity for all cases are shown in Figures (8-a,b,c,d) , (9-a,b,c,d) and (10-a,b,c,d) respectively.

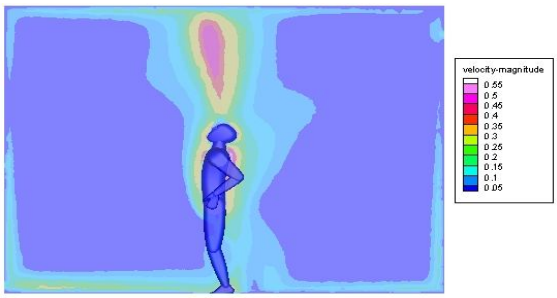

Figure8-a: Velocity contribution in the case 4

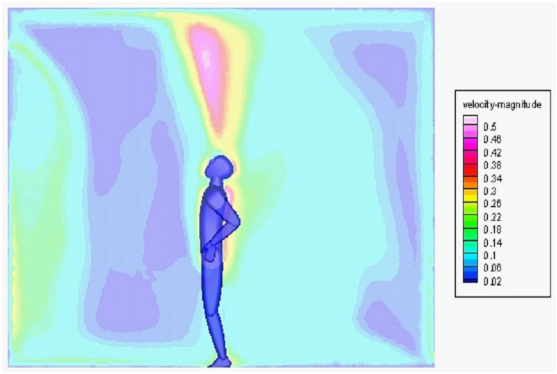

Figure8-b: Velocity contribution in the case 1

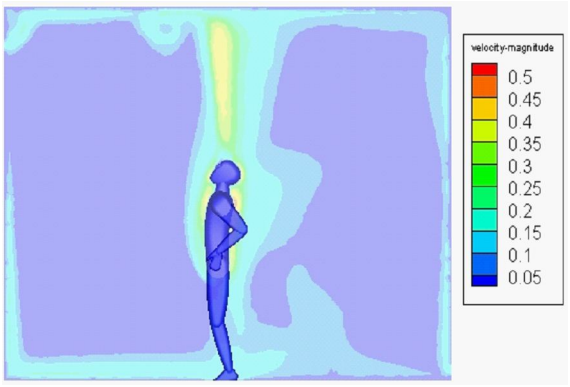

Figure8-c: Velocity contribution in the case 3

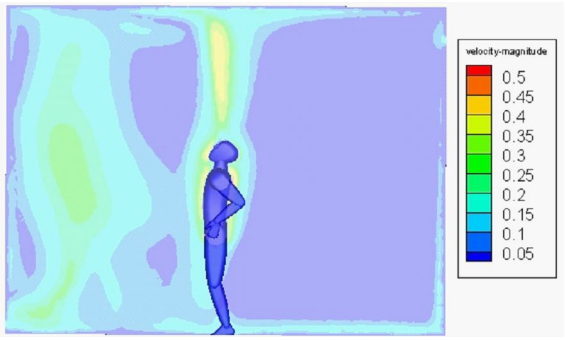

Figure8-d: Velocity contribution in the case 2

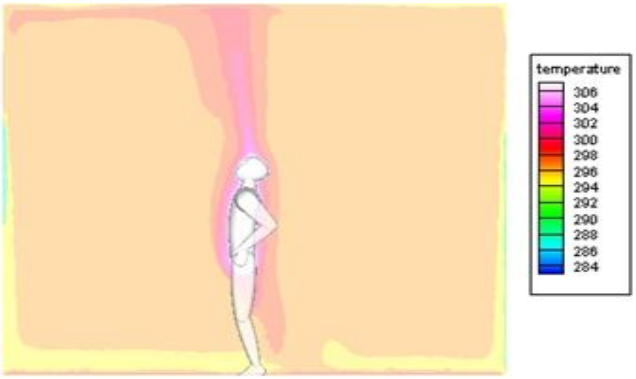

Figure9-a: Temperature contribution in the case 4

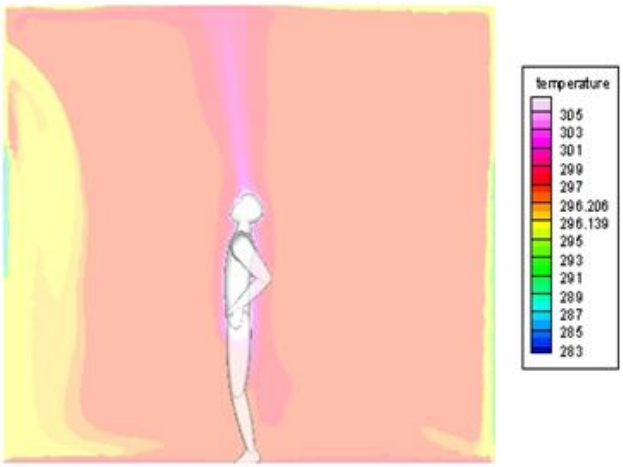

Figure9-b: Temperature contribution in the case 1

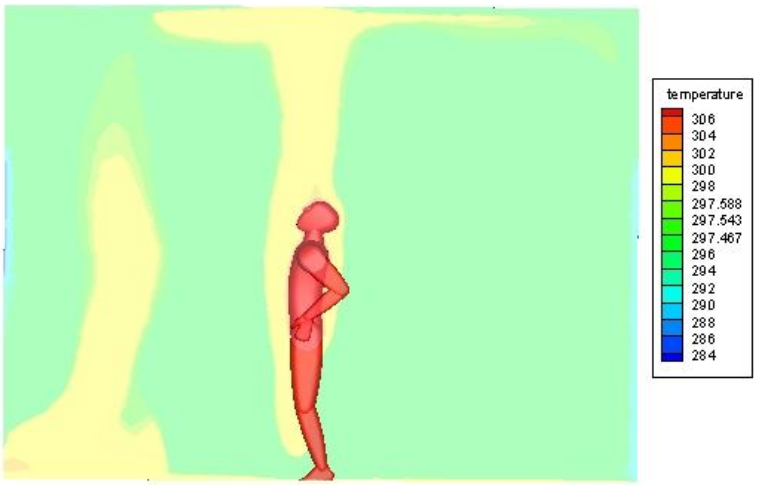

Figure9-c: Temperature contribution in the case 3

Figure9-d: Temperature contribution in the case 2

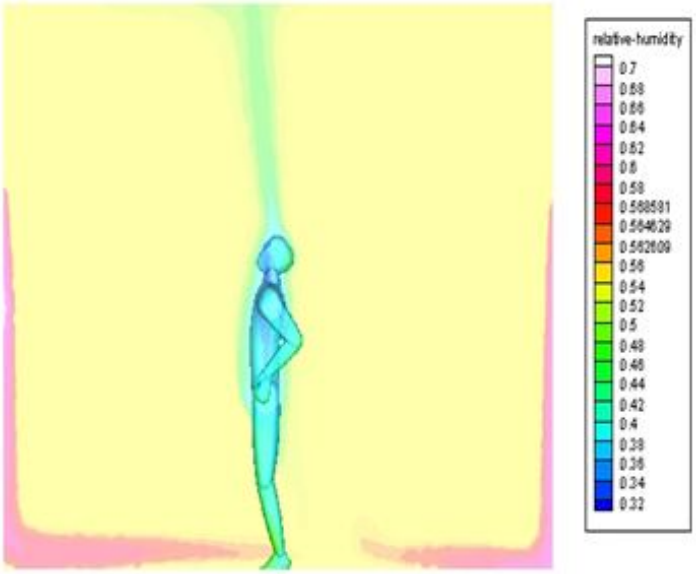

Figure10-a: Relative humidity contribution in the case 4

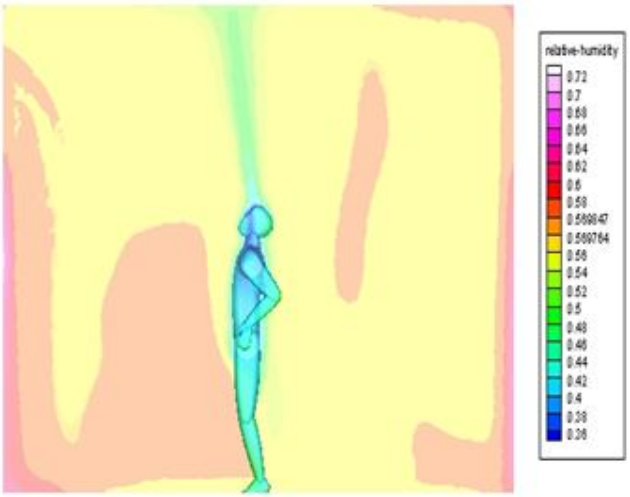

Figure10-b: Relative humidity contribution in the case 1

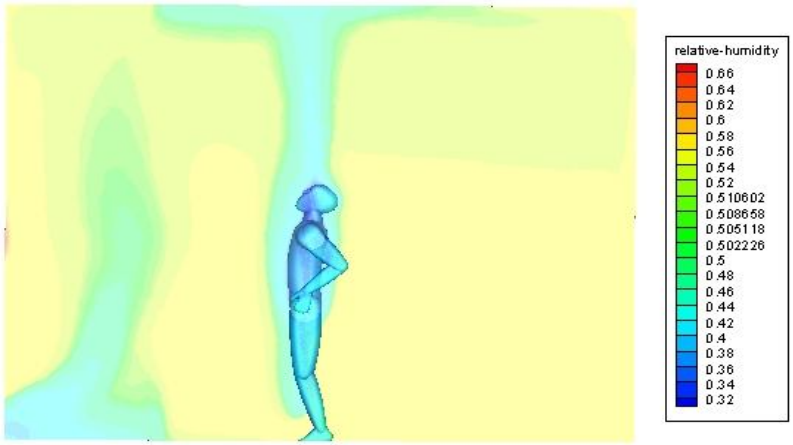

Figure10-c: T Relative humidity contribution in the case 3

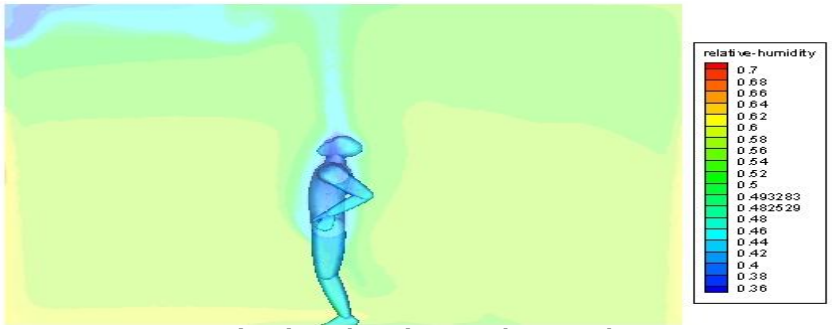

Figure10-d: Relative humidity contribution in the case 2

In all cases, the relative humidity when the inlet is located at the lowest level is in the standard range of ASHRAE (45 to 55). For wet climate zones, these conditions become worse, and the inlet with lower level is more suitable.

The effects of locating along the longitudinal direction on the results

In order to evaluate the locations of the vents along the longitudinal direction, the inlet and outlet locations have been analyzed in 6 different states. Figure 11 shows these states.

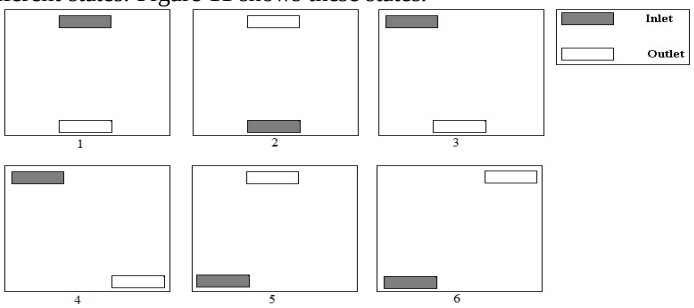

Figure11: the different states of the locations of the vents along the longitudinal direction

Studies have been carried out for the inlet air temperature of 22 ° C and air velocity of 0.15 m/s and the results are shown in Table 3. The results imply that there is no significant difference between the results for different states. The average maximum temperature difference between room temperature and mean average of radiation is less than 0.5 ° C and PMV in all six cases is almost identical. These results mean that in the residential room the inlet and outlet in the longitudinal direction, does not have any influence on thermal environment parameters, and its effect is restricted only to the velocity in regions adjacent to the side walls and this effect does not influence the thermal comfort.

The effects of locating along transverse direction on the results

Here we studied the effects of the location of the inlet and outlet vents on the side walls (case1) and on the opposite walls (case 2). For case 1, the air flow has asymmetrical distribution with improper velocity. This causes a decrease in the heat exchange between the body and the air. For case 2, there is no difference between the PMV in various states, but it makes asymmetric distribution of the heat flux out of the body while the total flux out of the body is constant. This causes the loss of the local heat comfort of the body. The problem has been solved at various inlet temperature and velocities for two cases. Table 5 shows the comparison between inlet and outlet modes (case1 and case2)

Table 5: The comparison between inlet and outlet modes in the same position in the front and side walls

	opposite walls			side walls		
Sample	22°C & 0.15 m/s	22°C & 0.5 m/s	22°C & 1 m/s	22°C & 0.15 m/s	22°C & 0.5 m/s	22°C & 1 m/s
T_{ave} °C	23.31	23.12	22.83	23.29	23.09	22.97
T_{mrt} °C	23.07	23.01	22.76	23.10	22.96	22.97
$Re\ Hu_{ave}$ %	54.57	54.45	54.79	55.57	55.5	55.66
$q_r\ W/m^2$	35.87	35.44	36.54	35.77	36.31	36.44
$q_c\ W/m^2$	43.63	49.23	54.17	44.10	48.24	53.91
$q_{res}\ W/m^2$	1.5	1.52	1.55	1.49	1.53	1.55
$E_{res}\ W/m^2$	5.19	5.25	5.30	5.15	5.24	5.28
$E_{sk}\ W/m^2$	30.99	35.11	35.02	31.09	34.64	34.49
PMV	0.6	0.89	1.16	0.62	0.92	1.2

With increasing the inlet velocity, the outlet flux of the body between losing its symmetry and discomfort will be increased even though according to the PMV the thermal comfort is provided. Figures (12-a,b,c,d,e,f) show the heat flux contours of the body's total output for three different inflow velocities and constant inlet air temperature of 22 ° C. The deviation from the equilibrium conditions has been increased with increasing the air velocity.

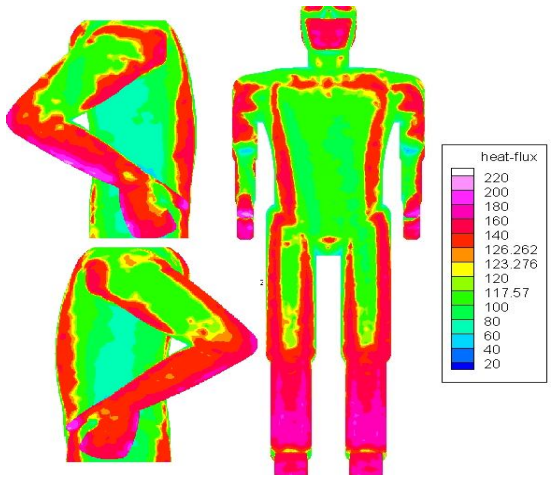

Figure 12.a: Heat flux contours of the body when the inlet is on the side wall & V= 0.15m/s

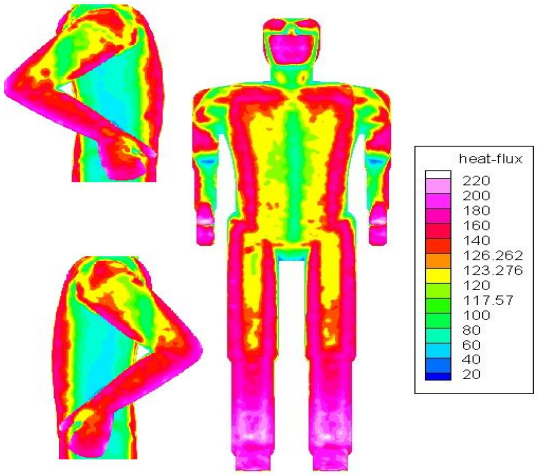

Figure 12.b: Heat flux contours of the body when the inlet is on the font wall & V= 0.15m/s

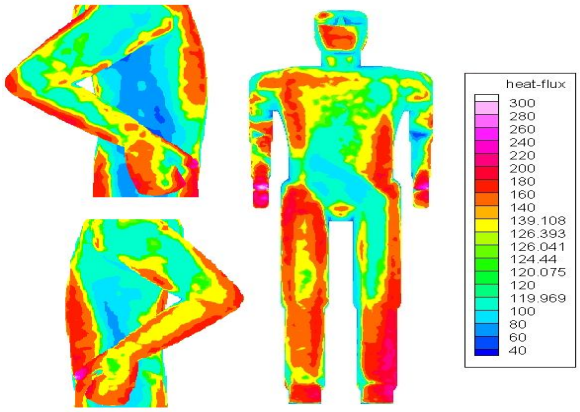

Figure 12.c: Heat flux contours of the body when the inlet is on the side wall & V= 0.5m/s

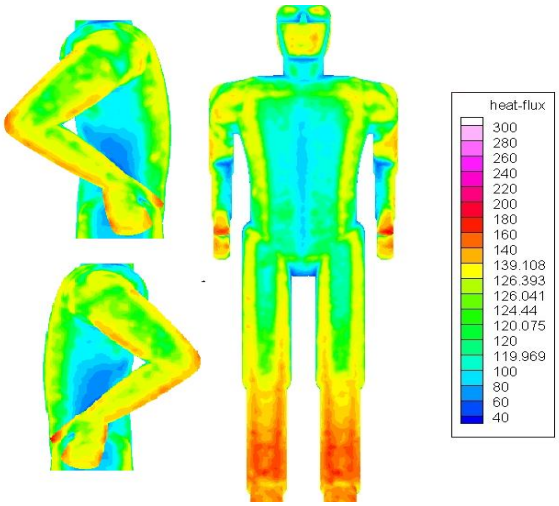

Figure 12.d: Heat flux contours of the body when the inlet is on the font wall & V= 0.5 m/s

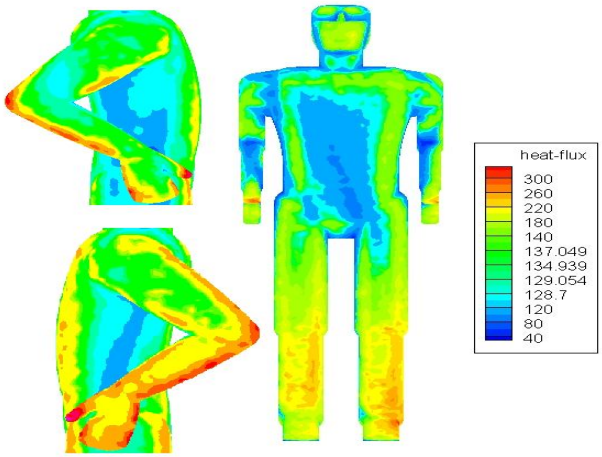

Figure 12.e: Heat flux contours of the body when the inlet is on the font wall & V=1.0 m/s

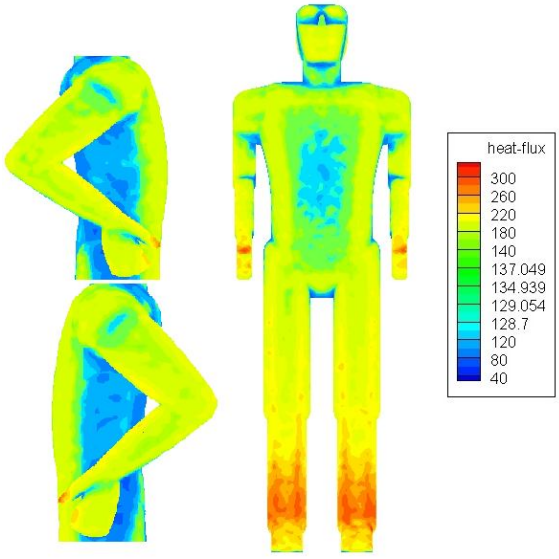

Figure 12.f: Heat flux contours of the body when the inlet is on the font wall & V= 1.0 m/s

The effect of inlet flow rate on thermal comfort and consumption of energy

After identifying a suitable location for placing of the inlet and outlet flow in the room, with increasing the flow rate at lower temperatures, the thermal comfort can be reached. This reduces the consumption of energy. Figure 13 shows the effects of changes in the air flow rate on PMV.

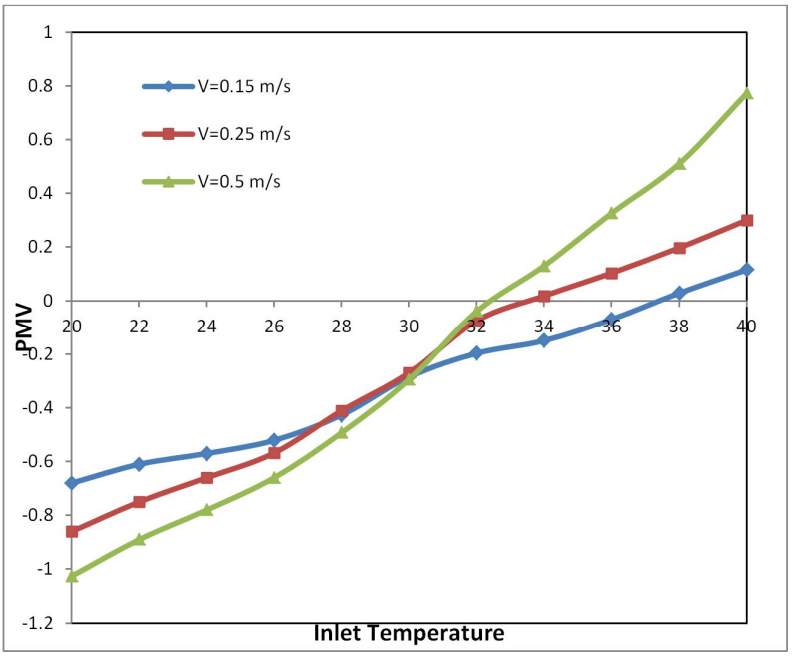

Figure 13: The effects of changes in air flow rate on thermal comfort index.

The results show that increasing the flow rate, increases the range of the PMV. In other words, at any temperature, with increasing the flow rate, the dissatisfaction will be increased. However, if this increase in constant temperature is negative in PMV values, this will cause a cooling sensation and if it is located in positive values, it will increase the feeling of heat. According to Figure 13, we have found that with increasing the inlet air flow rate, the inlet air temperature needed to reach thermal comfort will be decreased. This causes the relative humidity to be decreased and also the required velocity to be reduced to provide the thermal comfort. Moreover the energy consumption will be decreased.

Table 6 shows the inlet air temperature values, mean temperature of the room, relative volume-averaged humidity when PMV is zero for the different velocities.

Table 6: The effective parameter on the thermal comfort index PMV=0

V_{in} m/s	T_{in} °C	T_{ave} °C	Re_{ave} %
0.15	37	4	52.3
0.25	33.6	24.9	49.4
0.5	33	26.1	45.1

Table 7 shows the fraction of radiation and convection heat transfer and other losses in the heat flux of the body. With increasing the inlet velocity the fraction of the convection heat transfer has been increased and the fraction of radiation heat transfer has been decreased.

Table 7: the fraction of radiative and convective heat transfer in the total flux of the body

V_{in} m/s	q_{conv}	q_{rad}	q_{res}	E_{res}	E_{sk}
0.15	36.95%	33.56%	1.34%	4.35%	23.8%
0.25	37.94%	33.06%	1.29%	4.68%	23.03%
0.5	41.93	31.07%	1.14%	4.78%	21.08%

Conclusions

In this research, a CFD simulation for flow around a virtual manikin in a residential room was presented. According to the results, it is concluded that the inlet and outlet should not placed along a lateral or longitudinal direction. Also, to decrease the stagnation region the inlet and outlet should not be located at the same height

level. Moreover, to obtain the thermal comfort the inlet and outlet should be located on the opposite sides of the walls. This will also provide the local thermal comfort along with the symmetrical heat flux around the same segments of the body. Locating the inlet and outlet vents along the longitudinal direction does not influence the air flow distribution and the thermal comfort. The proper position for the inlet is along the vertical direction and at the lowest height level. This causes the relative humidity to be decreased and also the required velocity to be reduced to provide the thermal comfort. Moreover the energy consumption will be decreased. The lower velocity makes lower heat losses through the walls and the manikin segments up to 25 % which eventually reduces the energy consumption.

With the selection of proper location of inlet and outlet vents, variations of temperature and velocity cause significant effects on the thermal comfort and energy consumption. The inlet velocity increment causes the thermal comfort to be achieved at lower temperatures which in turn reduces the consumption of energy. Also, a better symmetrical velocity distribution around the manikin is also presented in this case

REFERENCES

[1] Nielsen P., Flow in air conditioned rooms (model experiments and solution of the flow equation). Danish Technical University, Copenhagen, Denmark, Thesis. 1974

[2] Gan G., Numerical Method for a full Assessment of indoor Thermal Comfort, International journal of indoor air quality and climate, Munksgaard, vol. 4, pp 154-168. 1994

[3] Murakami S , Kato S & Zeng J ,Flow and Temperature Fields Around Human Body with Various Room air distribution CFD study on Computational Thermal Manikin – Part I.ASHRAE Transactions , ashrae.org , vol. 103, pp 3-15. 1997

[4] Kurazumi Y., Tsuchikawa T., Yamato Y., Kakutani K., Matsubara N., Horikoshi T., The posture and effective thermal convection area factor of the human body, Japanese Journal of Biometeology 2003; 40(1) 3–13

[5] Tanabe S., Numerical Comfort Simulator for Evaluating Thermal Environment. Proceeding of the 10th International Conference on Environmental Ergonomics , Fukuoka , Japan ,pp 435-438. 2000

[6] kilic M., Sevilgen G.: Modeling airflow, heat transfer and moisture transport around a standing human body by computational fluid dynamics, International communication in Heat and Mass transfer 35 (2008) 1159-1164

[7] White F.M. 2006: Viscous fluid flow, 2nd ed, omide enghelab publication

[8] Batchelor, G. K. 1967, An Introduction to Fluid Dynamics. Cambridge Univ. Press. Cambridge, England

[9] Wyon D.P., Fanger P.O., Olesen , B.W., C.J.K. Pedersen, The mental performance of subjects clothed for comfort at two different air temperatures, Ergonomics 18 (1975) 358–374

[10] Barth T. J. and Jespersen D. The design and application of upwind schemes on unstructured meshes. Technical Report AIAA, 89-0366. AIAA 27th Aerospace Sciences Meeting, Reno, Nevada1989

[11] ASHRAE Handbook-Fundamental, American Society of Heating, Refrigeration and Air-Conditioning Engineers, Atlanta 2001.